Pore size is a critical parameter for obtaining sustained protein release from electrochemically synthesized mesoporous silicon microparticles

Ester Pastor, Elaine Reguera-Nuñez, Eugenia Matveeva, Marcos Garcia-Fuentes

Mesoporous silicon has become a material of high interest for drug delivery due to its outstanding internal surface area and inherent biodegradability. We have previously reported the preparation of mesoporous silicon microparticles (MS-MPs) synthesized by an advantageous electrochemical method, and showed that due to their inner structure they can adsorb proteins in amounts exceeding the mass of the carrier itself. Protein release from these MS-MPs showed low burst effect and fast delivery kinetics with complete release in a few hours. In this work, we explored how tailoring the size of the inner pores of the particles controls the protein release process. Three new MS-MPs prototypes were prepared by electrochemical synthesis, and the resulting carriers were characterized for morphology, particle size, and pore structure. MS-MPs had 90 μm mean particle size, and irregular morphology; depending on the current density applied, pore size changed between 5 and 13 nm. The model protein α-chymotrypsinogen was loaded into MS-MPs by adsorption and solvent evaporation. In the subsequent release experiments, no burst release of the protein was detected for any prototype. However, prototypes with larger pores (>10 nm) reached 100% release in 24-48 h, whereas prototypes with small mesopores (<6 nm) still retained most of their cargo after 96 h. The MS-MPs with ~6 nm pores were loaded with a protein of therapeutic interest, BMP7. Our results confirmed that these MS-MPs can provide up to two weeks of sustained release for BMP7 in its antigenically active form.

Pore size is a critical parameter for obtaining sustained protein release from electrochemically synthesized mesoporous silicon microparticles

E. Pastor [1], E. Reguera-Nuñez [2], E. Matveeva[1*], M. Garcia-Fuentes[2*]

[1] EM-Silicon Nanotechnologies S.L., Valencia, Spain

[2] Center for Research in Molecular Medicine and Chronic Diseases (CIMUS), Dep. Pharmacy and Pharmaceutical Technology, and Health Research Institute (IDIS), Campus Vida, Universidad de Santiago de Compostela, Spain

* Corresponding authors:

Dr. Eugenia Matveeva: eumat@em-silicon.com

Prof. Marcos Garcia-Fuentes: marcos.garcia@usc.es

11 **ABSTRACT**

12 Mesoporous silicon has become a material of high interest for drug delivery due to its outstanding
13 internal surface area and inherent biodegradability. We have previously reported the preparation
14 of mesoporous silicon microparticles (MS-MPs) synthesized by an advantageous electrochemical
15 method, and showed that due to their inner structure they can adsorb proteins in amounts
16 exceeding the mass of the carrier itself. Protein release from these MS-MPs showed low burst
17 effect and fast delivery kinetics with complete release in a few hours. In this work, we explored
18 how tailoring the size of the inner pores of the particles controls the protein release process.
19 Three new MS-MPs prototypes were prepared by electrochemical synthesis, and the resulting
20 carriers were characterized for morphology, particle size, and pore structure. MS-MPs had 90 μm
21 mean particle size, and irregular morphology; depending on the current density applied, pore size
22 changed between 5 and 13 nm. The model protein α-chymotrypsinogen was loaded into MS-MPs
23 by adsorption and solvent evaporation. In the subsequent release experiments, no burst release of
24 the protein was detected for any prototype. However, prototypes with larger pores (>10 nm)
25 reached 100% release in 24-48 h, whereas prototypes with small mesopores (<6 nm) still retained
26 most of their cargo after 96 h. The MS-MPs with ~6 nm pores were loaded with a protein of
27 therapeutic interest, BMP7. Our results confirmed that these MS-MPs can provide up to two
28 weeks of sustained release for BMP7 in its antigenically active form.

29 **Keywords:** mesoporous silicon; pore size; controlled release; microparticles; protein delivery;
30 Bone Morphogenetic Protein

1. INTRODUCTION

Mesoporous silicon (MS)-based materials are currently investigated in a variety of systems for drug delivery and tissue engineering applications (Anglin et al., 2008; Santos, 2014). Their main advantage lies on their outstanding surface area arising from the fine mesoporous structure that allows remarkable drug loadings to be achieved just by plain adsorption (Prestidge et al., 2008). MS is also biocompatible (Canham 1995; Godin et al., 2008; Salonen et al., 2008), and degrades in the body to silicates (SiO_2) (Canham 1995; Salonen et al,. 2008; Pastor et al., 2009) that are eliminated by renal excretion (Popplewell et al., 1998). Inspired by these properties, researchers have investigated silicon-based carriers in a variety of formats (i.e. scaffolds, microparticles, nanoparticles, etc.) for delivering hydrophobic and hydrophilic drugs (Anglin et al., 2008; Prestidge et al., 2008; Salonen et al., 2008). MS-based materials have also been proposed for delivering drug loaded nanoparticles within the concept of multistage delivery vehicles (Tasciotti et al., 2008).

Devices composed of a crystalline mesoporous silicon matrix are alternatives to silica mesoporous structures (Kresge et al., 1992), but unlike those, they do not require a mesophase template removal for their preparation. Mesoporous silicon can be prepared by stain-etching or electrochemical anodizing of silicon. Both methods result in suitable mesoporous (nanostructured) materials, but the stain-etching method is less controlled with respect to pore homogeneity, and often leaves an untreated crystalline silicon core inside the particles. Medical materials prepared from stain-etched mesoporous silicon should be additionally checked for complete removal of toxic nitric oxide residues. The electrochemical method for MS production is therefore more medical-friendly, and recently its scalability has been considerably improved (Makushok, Matveyeva & Pastor, 2012).

54 The desired nanostructure of MS fabricated by electrochemical methods can be easily achieved
55 by a simple tuning of the preparation conditions, first of all, the applied current density. Even
56 though these inner nanostructure parameters (pore size, overall porosity, particle size, etc.) are
57 important for MS silicon drug carriers, they cannot assure optimal drug payloads juts by
58 themselves. The interaction between the drug and the carrier surface needs also to be engineered,
59 and thus the surface modification and functionalization of MS nanostructures has been
60 extensively studied in recent years (Jarvis, Barnes & Prestidge, 2011; 2012; Barnes, Jarvis &
61 Prestidge, 2013). Among different techniques, a simple oxidation is frequently performed that
62 converts the outer surfaces of crystalline mesoporous silicon to a mesoporous silica replica
63 (Kresge et al., 1992).
64 In a previous publication from our group, MS microparticles (MS-MPs) with an average pore size
65 of 35 nm were prepared by an electrochemical method and stabilized by thermal oxidation. These
66 MS-MPs were successfully loaded with two model proteins, insulin and bovine serum albumin
67 BSA (Pastor et al., 2011). Although these proteins were released from a vehicle in a controlled
68 manner, the process was fast (~80-100% release in less than 2 h), and consequently only suitable
69 for some applications such as mucosal drug delivery.
70 Previous studies with hydrogels (Peppas et al., 2000), solid polymers (Sandor et al., 2001), and
71 other mesoporous materials (Santos, Radin & Ducheyne, 1999) have shown that modulation of
72 the inner nanostructure of the carrier can change the kinetics of drug release. We proposed that
73 similar principles should apply for controlling the release of proteins from electrochemically
74 synthesized MS-MPs. To address this hypothesis, we prepared MS-MPs with different pore sizes
75 and explored how changes in inner nanostructure can influence the release of loaded proteins.
76 This study was performed initially with the model protein α-chymotrypsinogen (aCT); then,
77 considering the bioactivity of MS materials for orthopedic regeneration (Canham, Reeves &

78 Newey, 1999; Pastor et al., 2007; Sun et al., 2007), we loaded a protein of therapeutic interest for
79 this application, bone morphogenetic protein-7 (BMP7).

2. MATERIALS AND METHODS

2.1. Materials

Boron doped silicon with different resistivity, 0.01–0.02 and 10-20 Ω·cm, was purchased from Si Materials (Germany); wafer diameter was 100.0 ± 0.5 mm and thickness of 525 ± 25 μm (pI = 2–3.5). Fluoric acid (HF) (48 %) was purchased from Riedel de Haën (Germany) and ethanol (96%) from Panreac (Spain). Synthetic air (N_2 with 21% of O_2) was provided from AbelloLinde S.A. (Spain). Avidin-peroxidase conjugate, α-chymotrypsinogen A (aCT) from bovine pancreas (pI = 9.5; Mw = 25.7 kDa), and 2,2'-azino-bis(3-ethylbenzthiazoline-6-sulfonic acid) were obtained from Sigma Aldrich (Spain). Recombinant human Bone Morphogenetic Protein-7 (BMP7) (pI = 8.1; Mw = 28.8 kDa), polyclonal antibody rabbit anti-human BMP7, and biotinylated polyclonal antibody rabbit anti-human BMP7 were purchased from PeproTech (UK). All other solvents and chemicals used were high-grade purity.

2.2. Preparation of mesoporous silicon microparticles (MS-MPs)

MS-MPs were obtained by an electrochemical method similar to that previously described by us (Pastor et al., 2009). The main difference was the use of a 1:1 HF:Ethanol electrolyte, and special cyclic regimes with etch-stops in order to improve the homogeneity of pore sizes distribution along with the in-depth etching (Bychto et al., 2008). A constant current step (40 or 60 mA/cm^2 for 5-10 s) was followed by an etch-stop step (no current applied for 2-5 s) in cyclic periods. After obtaining a MS layer of ~150 μm thickness, the electrochemical process was stopped, and the Si wafer was washed thoroughly with distilled water, dried, and the porous material was scratched from the remaining Si substrate. The obtained MS was subjected to a thermal oxidation under a flow of synthetic air for 1 hour at 500 or 650 ºC (Programat P200 equipped with a vacuum pump VP3 and gas inlet, Ivoclar-Vivadent, Inc., US). To reduce the particle size to the

103 micrometer scale, the MS material was milled and sieved in cascade. The fraction between 75
104 and 100 μm was selected for further studies. Henceforth, this fraction is referred to as MS-MPs.
105 The preparation conditions for the three different MS-MP prototypes studied in this work are
106 summarized in Table 1. For example, prototype B was prepared from Si wafer of 0.01-0.02 Ω·cm
107 resistivity, under a current density of 40 mA/cm^2 applied for 10 s, and then interrupted by a 2 s
108 interval of zero current (etch-stop). This regime was cyclically repeated for a few hours until the
109 150 micron porous layer was grown. After recollecting the porous material, the material was
110 thermally oxidized at 650 for one hour.

111 *2.3. Characterization of MS-MPs*

112 The porosity of the porous silicon materials was determined gravimetrically by comparing the
113 mass of the silicon wafer before and after anodizing as previously described (Pastor et al., 2011).
114 Particle sizes were analyzed with a Mastersizer 2000 (Malvern Instruments, UK). MS-MPs
115 morphology was visualized by high resolution Scanning Electron Microscopy (SEM, Hitachi
116 S4500, Japan). Additionally, the Brunauer- Emmett-Teller (BET) surface area of the MS-MPs
117 was determined by N_2 adsorption–desorption isotherms (Micrometrics ASAP 2020 V3.04H,
118 Micromeritics France S.A., France). Pore size was calculated from the same N_2 adsorption data,
119 by the Barroett-Joyner-Halenda (BJH) method.

120 *2.4. Protein loading*

121 Protein loading was carried out by solvent evaporation (Prestidge et al., 2008). Briefly, 20 μL of
122 the model protein aCT (3 mg/mL) or BMP7 (5 μg/mL) in aqueous solutions were added to a
123 fixed amount of MS-MPs (1 mg). The samples were gently vortexed for 10 seconds, and then
124 incubated under mild agitation at 37 ºC until total evaporation of solvent was reached and all
125 amounts of proteins incorporated into the MS-MPs (about 7 hours). The final protein loadings

126 were: 60 μg/mg of MS-MPs for aCT, and 0.1 μg/mg of MS-MPs for BMP7. Loaded MS-MPs
127 were freeze-dried and stored at -20 ºC until use.

128 *2.5.* In vitro *release studies*

129 Samples comprising 1 mg of MS-MPs loaded with aCT or BMP7 were incubated with 500 μL of
130 PBS (pH 7.4) under agitation (100 rpm, Heindolf, Titramax 1000, Germany) at 37 ºC (Heindolf,
131 Inkubator 1000, Germany). At scheduled time points, release samples were collected, and
132 centrifuged at 7000 RCF for 10 min at 4 ºC (Beckman Coulter, Microfuge 22R). The amounts of
133 aCT in supernatants were determined by the bicinchoninic acid method (Micro BCA protein
134 Assay Kit, Pierce Biotechnology Inc., USA), and those of BMP7 by ELISA, as previously
135 reported by us (Reguera-Nuñez et al., 2014). Amounts of released protein are expressed as
136 percentage of a total protein mass added at the loading stage since the whole mass was
137 considered as absorbed upon solvent evaporation. This consideration was proved to be a
138 reasonable approximation since the detected 2-week release was >70% for aCT and >60% for
139 BMP7 (see section 3.3 and 3.4).
140

3. RESULTS AND DISCUSSION

3.1 Characterization of different MS-MPs carriers

Mesoporous silicon microparticles (MS-MPs) were prepared by electrochemical etching, thermal stabilization, and milling to reduce the particle sizes. The resulting powder was sorted by sieving. The particles of the selected fraction (i.e. the MS-MPs) were irregular in shape, but homogeneous in size (Fig. 1A). All the MS-MPs prototypes generated showed a normal distribution of sizes with a mean value around 90 μm (Figure 1B). This normal particle distribution contrasted with our previous data where the particle distribution was log-normal (Pastor et al., 2011). This might be related to the different particle fractions selected on each work (90 μm vs 33 μm mean size, respectively). The mesoporous structure of MS-MPs observed by high resolution SEM (Fig. 1C) revealed the regular and homogeneous pores propagated along a single direction, as it is common for electrochemically prepared MS. The SEM analysis, however, might not reveal the smallest pores of the materials due their well-known resolution limits.

The inner structure for three different MS-MP prototypes (A-C) prepared under the conditions summarized in Table 1 was characterized by N_2 adsorption-desorption experiments (Fig. 1D). The data revealed very high specific surface areas for prototypes A and B (>200 m^2/g), but even more for prototype C (350 m^2/g). The porosity of all samples was high (>50%), and the mean pore diameter was ~12 nm for prototypes A and B, and ~6 nm for prototype C. These pore sizes were significantly smaller than MS-MPs prepared in our previous work (Pastor et al., 2011), a result of the different preparation conditions. Due to their tighter internal structure, we expected that the MS-MPs obtained in this work would be more suitable for the sustained release of proteins.

Due to the limited number of prototypes studied and the important difference in parameters observed, it is difficult to draw unequivocal conclusions on the relationships between the MS-MPs preparation parameters (Table 1) and the resulting carrier properties (Table 2). Still, under the tested preparation conditions, there is a positive correlation between the current density and the specific surface area. Also, an inverse correlation between the applied current density and the mean pore diameter can be noted, although the doping level of Si wafer might play a dominant role in this correlation. Globally, the study confirms the possibility to prepare MS-MPs with controllable mesoporous inner structures by the electrochemical method.

3.2. Protein loading in MS-MPs

For protein loading in this work we decided to work under forcing conditions, and we evaporated a protein solution in the presence of the MS-MPs at 37ºC. This method has the main advantage of forcing protein encapsulation, which can be assumed to be close to 100%. As we will see from the protein release experiments, this is a safe assumption under the conditions tested.

When using this loading method, the mechanisms that drive protein loading would be capillary forces and adsorption from a continually concentrating solution (Karlsson et al., 2003). Other possible mechanisms would be electrostatic interactions; after thermal oxidation the MS-MPs surface bears a negative charge as the silicon oxides cover the entire porous network (Zangooie, Bjorklund & Arwin, 1998). This might affect the loading and release of cationic proteins such as aCT and BMP7. Under the tested conditions, the final protein payloads were 60 µg for aCT and 0.1 µg for BMP7 per mg of the carrier.

3.3 Pore size can control the release of a model protein (aCT) from MS-MPs

The release of loaded aCT from the three MS-MPs prototypes was analyzed *in vitro* (PBS, 37ºC). No burst release was observed for any of the tested prototypes, suggesting that most

187 protein is inside the pores and not adsorbed on the outer MS-MP surface (Fig. 2A). This
188 behavior is in agreement with our previous study on insulin and BSA, where despite of a faster
189 release (<2 h), only a moderate burst effect was observed (~30%) (Pastor et al., 2011). In the
190 present work, the burst effect was drastically reduced, presumably because of lower pore size of
191 carriers, and because of the different procedures for protein loading (solvent evaporation vs.
192 adsorption equilibria).
193 The MS-MPs investigated in this work were able to control protein release for longer periods of
194 time than the carriers previously reported by us (Pastor et al., 2011): for prototypes A and B a
195 ~100% release was achieved in 30-40 h after incubation at 37ºC in PBS. Prototype C showed
196 even more sustained kinetics with high retention of aCT still after 96 h (Fig. 2A). However, after
197 2-weeks, sample C had released a 77.2% ± 4.2 (n=3) of the loaded aCT. The slower release
198 should be associated with the nanostructure of the carriers, mainly to their pore size. Mean pore
199 size was <15 nm for all prototypes studied here, and 33 nm in our previous work. Prototype C
200 possesses pores with a mean size of ~6 nm, half of those of prototypes A and B, and similar to
201 the radius of gyration of aCT (1.76 nm, (Perkins et al., 1993)). As observed in other systems
202 (Santos, Radin & Ducheyne, 1999; Peppas et al., 2000; Sandor et al., 2001), when the drug's
203 radius of gyration is about the size of pores in the matrix, diffusion might be hindered, and more
204 sustained release kinetics achieved. When comparing the different prototypes studied in this
205 work, particle inner structure seems to be the critical factor modulating different release kinetics.
206 When comparing the performance of the MS-MP prototypes from this work with those of our
207 previous work (Pastor et al., 2011), two additional factors need to be considered. First, the effect
208 of the chemical differences of the proteins tested: insulin and BSA, used before, both bear
209 negative charges in PBS, but aCT is positive and, therefore, more amenable to an ionic
210 interaction with silicon oxide. Another parameter that could have some limited influence on
211 protein release is the average particle dimensions, which was 33 μm in our previous work, and is

90 μm here (Pastor et al., 2011). Particle dimension will influence the diffusion length within the carrier for the protein. Recently, a new production method yielding planar mesoporous silicon microparticles with a controlled thicknesses, porosity and pore sizes has been reported (Makushok, Matveyeva & Pastor, 2012; E. Matveeva, unpublished data). This new kind of materials might be interesting for release mechanism studies since in those, the lateral dimensions, perpendicular to the pore axis, will play no important role in the release process.

3.4 MS-MPs can achieve a 2-week sustained release of antigenically active BMP7

Based on promising data obtained with aCT protein, we tested MS-MP prototype C for the controlled release of a therapeutic protein: BMP7. This protein is approved by FDA and other regulatory agencies for orthopedic applications (OP-1 Putty and OP-1 Implant, Stryker, US), and it is delivered through a collagen sponge with limited controlled release properties. This limited controlled release has been linked to most of the treatment undesirable effects (Lane, 2001). MS-MPs were loaded with BMP7 as described in section 3.2, and the release kinetics was analyzed. Consistently with the data obtained with aCT, a 2-week sustained release was achieved (Fig. 2B). Once again, the release kinetics was characterized by low burst (<10%), and by a sustained release profile for at least 14 days. Maximum release observed over the experiment (28 days) was ~70%. It is important to note that the quantification of BMP7 in the supernatant was performed by ELISA, and thus, it guarantees the presence of the protein in its antigenically-active form upon release.

The release profile was fitted to zero-order, first-order, Higuchi and to the Kosmeyer-Peppas models (Wizard - Statistics, Visualization, Data Analysis, Predictive Modeling, version 1.4, Evan Miller©, US). Fitting to the first-order and Higuchi models was adequate ($p<0.008$ and $p<0.002$, respectively), but the best fit was achieved with the Kosmeyer-Peppas model (BMP released%$=10.4 \cdot t\,(\text{days})^{0.64}$, $p<0.001$). The Kosmeyer-Peppas model is effective to describe

236 release systems where release kinetics might depend on several factors. The diffusional
237 exponent (n=0.64) indicates a process of anomalous diffusion (Korsmeyer et al., 1983; Peppas,
238 1985).
239 The similarities between aCT and BMP7 release kinetics reflect their similar physicochemical
240 properties. Indeed, BMP7 has a radius of gyration ~3.5 nm (by analogy with other BMPs, (Berry
241 et al., 2006)) just slightly larger than aCT. It has also a basic isoelectric point (8.1) close to that
242 of aCT (9.5). These similarities result in consistent profiles for both proteins, and suggest the
243 robustness of the delivery technology.
244 In summary, we have achieved sustained release of BMP7 for at least two weeks by using
245 electrochemically synthesized MS-MPs. A preparation technology for the whole therapeutic
246 system is convenient, since both components, protein solution and pre-formed empty MS-MPs,
247 can be integrated together in an extemporaneous process. Due to the recently reported
248 osteointegration properties of the MS-MP carrier itself (Sun et al., 2007), one of the immediate
249 promising applications of this system would be in the bone regeneration area.

250 **4. CONCLUSIONS**

251 Mesoporous silicon microparticles with controlled inner structure (pore size) can be prepared by
252 an electrochemical method, and loaded with proteins by simple adsorption and solvent
253 evaporation. Under optimized electrochemical conditions these microparticles present a
254 nanostructure with pore sizes below 10 nm, and provide controlled release of proteins that can
255 last several days. The medical potential of the electrochemically synthesized mesoporous silicon
256 microparticles has been established by showing a two weeks sustained release of bone
257 morphogenetic protein BMP7.

5. ACKNOWLEDGMENTS

We thank Vika Makushok (EM Silicon Nanotechnology S.L.) for technical help on MS-MP sample preparation and characterization, and Lidia Pereiro and Mariana Landin (University of Santiago de Compostela) for technical help on N_2 adsorption-desorption experiments.

6. REFERENCES

Anglin EJ, Cheng L, Freeman WR, Sailor MJ (2008). "Porous silicon in drug delivery devices and materials." Advanced Drug Delivery Reviews **60**: 1266-1277.

Barnes TJ, Jarvis KL, Prestidge CA (2013). "Recent advances in porous silicon technology for drug delivery." Therapeutic Delivery **4**(7): 811-823.

Berry R, Jowitt TA, Ferrand J, Roessle M, Grossmann JG, Canty-Laird EG, Kammerer RA, Kadler KE, Baldock C (2006). "Role of dimerization and substrate exclusion in the regulation of bone morphogenetic protein-1 and mammalian tolloid." Proceedings of the National Academy of Sciences **106**: 8561–8566.

Bychto L, Makushok Y, Chirvony V, Matveeva E (2008). "Pulse electrochemical method for porosification of silicon and preparation of porous Si dust with controllable particle size distribution." Physica Status Solidi (c) **5**(12): 3789–3793.

Canham LT (1995). "Bioactive silicon structure fabrication through nanoetching techniques." Advanced Materials **7**: 1033-1037.

Canham LT, Reeves CL, Newey JP (1999). "Derivatized mesoporous silicon with dramatically improved stability in simulated human blood plasma." Advanced Materials **11**: 1505-1507.

Godin B, Gu J, Serda RE, Ferrati S, Liu X, Chiappini C, Tanaka T, Decuzzi P, Ferrari M (2008). "Multistage Mesoporous Silicon-based Nanocarriers: Biocompatibility with Immune Cells and Controlled Degradation in Physiological Fluids." Controlled Release Newsletter **25**: 9-11.

Jarvis KL, Barnes TJ, Prestidge CA (2011). "Surface chemical modification to control molecular interactions with porous silicon." Journal of Colloid and Interface Science **363**(1): 327-333.

Jarvis KL, Barnes TJ, Prestidge CA (2012). "Surface chemistry of porous silicon and implication for drug encapsulation and delivery applications." Advances in Colloid and Interface Science **175**: 23-38.

Karlsson LM, Tengvall PLundstrom I, Arwin H (2003). "Penetration and loading of human serum albumin in porous silicon layers with different pore sizes and thicknesses." Journal of Colloid and Interface Science **266**: 40–47.

Korsmeyer RW, Gurny R, Doelker E, Buri P, Peppas NA (1983). "Mechanisms of solute release from porous hydrophilic polymers." International Journal of Pharmaceutics **15**(1): 25-35.

Kresge CT, Leonowicz ME, Roth WJ, Vartuli JC, Beck JS (1992). "Ordered mesoporous molecular sieves synthesized by a liquid-crystal template mechanism." Nature Materials **359**: 710-712.

Lane JM (2001). "BMPs: Why Are They Not in Everyday Use? ." The Journal of Bone & Joint Surgery **83**(1): S161-162.

Makushok Y, Matveyeva Y, Pastor GEL (2012). Nanostructured semiconductor materials, method for the manufacture thereof and current pulse generator for carrying out said method WO2012065825A3.

Pastor E, Matveeva E, Parkhutik V, Curiel-Esparza J, Millan MC (2007). "Influence of porous silicon oxidation on its behaviour in simulated body fluid." Physica Status Solidi (c) **4**: 2136–2140.

Pastor E, Matveeva E, Valle-Gallego A, Goycooea FM, Garcia-Fuentes M (2011). "Protein delivery based on uncoated and chitosan-coated mesoporous silicon microparticles." Colloids and Surfaces B: Biointerfaces **88**: 601– 609.

Pastor E, Salonen J, Vesa-Pekka LehtoV-P, Matveeva E (2009). "Electrochemically induced bioactivity of porous silicon functionalized by acetylene." Physica Status Solidi (a) **206**(6): 1333-1338.

Peppas NA (1985). "Analysis of Fickian and non-Fickian drug release from polymers." Pharmaceutica Acta Helvetiae **60**: 110-111.

310 Peppas NA, Bures P, Leobandung W, Ichikawa H (2000). "Hydrogels in pharmaceutical
311 formulations." European Journal of Pharmaceutics and Biopharmaceutics **50**(1): 27-46.
312 Perkins SJ, Smith KF, Kilpatrick JM, Volanakis JE, Sim RB (1993). "Modelling of the serine-
313 proteinase fold by X-ray and neutron scattering and sedimentation analyses: occurrence of the
314 fold in factor D of the complement system." Biochemical Journal **295**: 87-99.
315 Popplewell J, King S, Day JP, Ackrill P, Fifield LK, Cresswell RG, di Tada ML, Liu K (1998).
316 "Kinetics of uptake and elimination of silicic acid by a human subject: a novel application of
317 32Si and accelerator mass spectrometry." Journal of Inorganic Biochemistry **69**: 177-180.
318 Prestidge CA, Barnes TJ, Mierczynska-Vasilev A, Kempson I, Peddie F, Barnett C (2008).
319 "Peptide and protein loading into porous silicon wafers." Physica Status Solidi (a) **205**: 311-
320 315.
321 Reguera-Nuñez E, C. Roca C, Hardy E, de la Fuente M, Csaba N, Garcia-Fuentes M (2014).
322 "Implantable controlled release devices for BMP-7 delivery and suppression of glioblastoma
323 initiating cells." Biomaterials **35**(9): 2859–2867.
324 Salonen J, Kaukonen AM, Hirvonen J, Lehto V-P (2008). "Mesoporous Silicon in Drug Delivery
325 Applications." Journal of Pharmaceutical Sciences **97**: 632–653.
326 Sandor M, Enscore D, Weston P, Mathiowitz E (2001). "Effect of protein molecular weight on
327 release from micron-sized PLGA microspheres." Journal of Controlled Release **76**(3): 297-
328 311.
329 Santos EM, Radin S, Ducheyne P (1999). "Sol–gel derived carrier for the controlled release of
330 proteins." Biomaterials **20**(18): 1695–1700.
331 Santos HA (2014). Porous silicon for biomedical applications, Woodhead Publishing.
332 Sun W, Puzas JE, Sheu TJ, Liu X, Fauchet PM (2007). "Nano- to Microscale Porous Silicon as a
333 Cell Interface for Bone-Tissue Engineering." Advanced Materials **19**: 921–924.

334 Tasciotti E, Liu X, Bhavane R, Plant K, Leonard AD, Price BK, Cheng MM-C, Decuzzi P, Tour
335 JM, Robertson F, Ferrari M (2008). "Mesoporous silicon particles as a multistage delivery
336 system for imaging and therapeutic applications." Nature Biotechnology **3**: 151-157.
337 Zangooie S, Bjorklund R, Arwin H (1998). "Protein adsorption in thermally oxidized porous
338 silicon layers." Thin Solid Films **313-314**: 825-830.

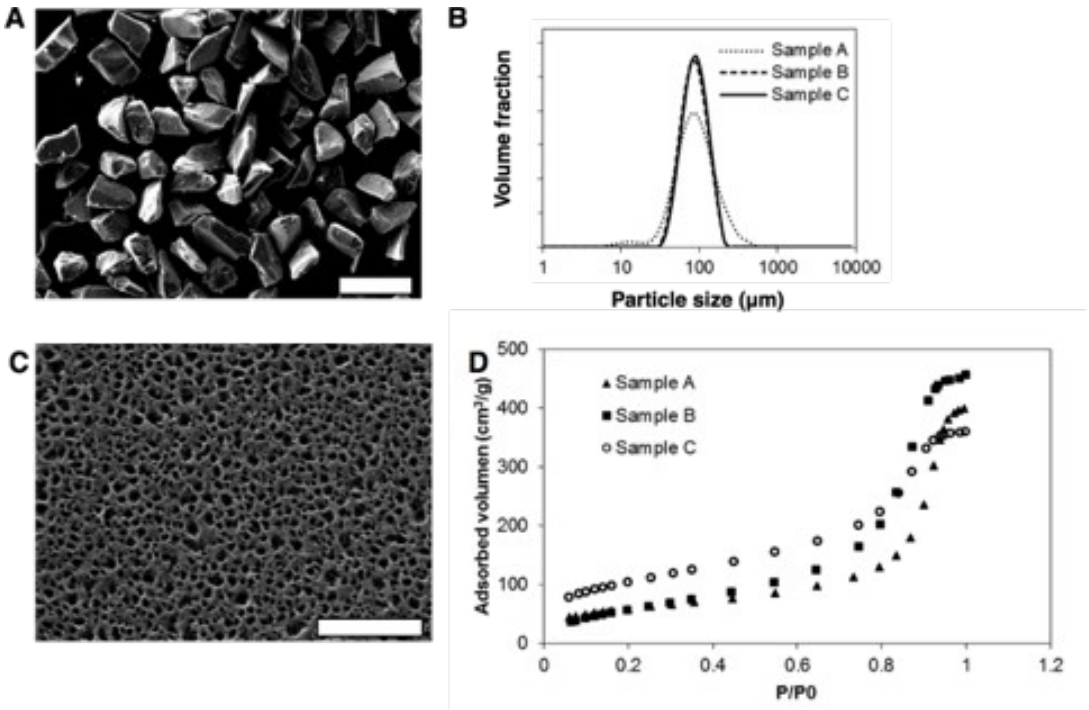

339 Figure 1. Morphological and physicochemical properties of mesoporous silicon microparticles (MS-MPs):
340 A) SEM image of MS-MPs (bar is 200 µm); B) Particle size distribution of the different MS-MP
341 prototypes measured with a particle size analyzer; C) Example of a SEM image of the surface of MS-MPs
342 (corresponding to prototype A, bar is 800 nm); D) N_2 adsorption isotherms, volume adsorbed vs. relative
343 pressure (P/P_0), for the different MS-MP prototypes.

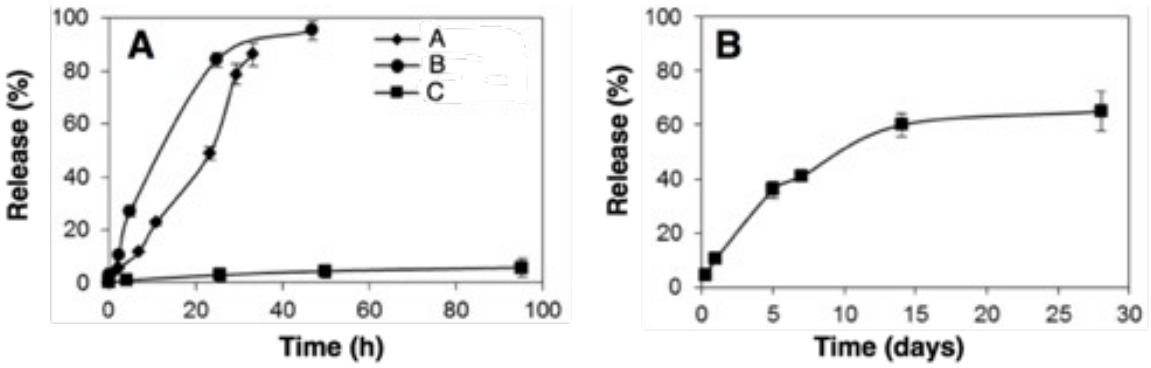

344 Figure 2. *In vitro* release profile of (A) α-chymotrypsinogen and (B) BMP-7 from MS-MPs prepared by

345 the electrochemical method. Data represent means ± S.D., n =3.

346 Table 1. Preparation conditions for different mesoporous silicon prototypes synthesized by the
347 electrochemical method under special cyclic regimes with etch-stop (zero current) applied after each
348 anodizing interval. Three different prototypes (A-C) were prepared and tested in this study, differing in
349 silicon waver resistivity, current densities, etch-stop times, and thermal oxidation temperatures.

Prototype	Si wafer resistivity (Ωcm)	Current density (mA/cm^2)/ anodizing time (s)	Etch stop time (s)	Oxidation temperature (ºC)
A	0.01-0.02	40 / 5	5	500
B	0.01-0.02	40 / 10	2	650
C	10-20	60 / 5	2	550

350 Table 2. Characteristics of the different mesoporous silicon microparticle prototypes.

Prototype	Specific surface (m^2/g)	Porosity (%)	Pore diameter (nm)
A	210.2	72	11.4
B	224.9	53	12.4
C	350.8	60	5.8